Electrokinetic leakage as a tool to probe internal fouling in MF and UF membranes

C. Rouquie, S. Liu, Murielle Rabiller-Baudry, A. Riaublanc, M. Frappart, Estelle Couallier, Anthony Szymczyk

Electrokinetic leakage as a tool to probe internal fouling in MF and UF membranes

C. Rouquié[1,2,3], S. Liu[2,4], M. Rabiller-Baudry[1], A. Riaublanc[3], M. Frappart[2], E. Couallier[2]*, A. Szymczyk[1]*

[1] Univ Rennes, CNRS, ISCR (Institut des Sciences Chimiques de Rennes) – UMR 6226, F-35000 Rennes, France

[2]CNRS, GEPEA, Université de Nantes, 37 Boulevard de l'université, BP 406, 44602Saint-Nazaire cedex, France

[3]INRA, BIA, Rue de la Géraudière, BP 71627, 44 316 Nantes Cedex 3, France

[4]ADEME, 20 avenue du Grésillé, BP90406, 49004 Angers cedex 01, France

*Corresponding authors: anthony.szymczyk@univ-rennes1.fr, estelle.couallier@univ-nantes.fr

Abstract

Tangential electrokinetic measurements are widely used to characterize membrane fouling as the membrane zeta potential is partly governed by the presence of foulant materials on its surface. However, in the case of porous materials as micro- (MF) and ultrafiltration (UF) membranes, a part of the streaming current flows through the porosity of the membrane during measurements. This electrokinetic leakage, is directly impacted by the presence of foulant materials inside the membrane porosity. Hence, this paper investigates for the first time the possibility of using electrokinetic leakage as a probe for detecting internal fouling, taking lipid fouling as example. Firstly, a lab-scale methodology combining "upside-down" fouling experiments with electrokinetic measurements demonstrated that the intensity of the electrokinetic leakage was related to the presence of internal fouling. Secondly, the concept was applied to the pilot-scale MF and UF of an oil-in-water emulsion

under various transmembrane pressures (TMP). A significant impact of the TMP on the internal fouling of a MF PES membrane was highlighted, whereas almost no impact of the TMP was noticed in the case of an UF PAN membrane. The developed methodology using the quantification of the electrokinetic leakage phenomenon allows distinguishing the contributions of internal and external (surface) fouling. These findings offer new application of tangential electrokinetic measurements to gain more insight into the characterization of membrane fouling.

Highlights:

- New characterization of internal fouling by tangential electrokinetic measurement
- Internal and external fouling contributions to membrane electrokinetic properties
- Impact of the operating transmembrane pressure on internal fouling occurrence

Keywords: Membrane fouling; electrokinetics; streaming current; microfiltration; ultrafiltration

1 Introduction

Despite the many advantages and applications of membrane filtration, performances keep being hampered by membrane fouling due to deposit and/or adsorption of compounds on the membrane surface and/or inside the membrane porosity. In the light of this, there is an important need of characterization methods in order to strengthen membrane fouling comprehension and thus improve fouling control during large-scale filtrations.

Many strategies have been applied so far to characterize membrane fouling, starting with conventional flux/pressure monitoring often combined with prediction or comprehension models (resistance-in-series, pore blocking, inertial lift models, etc.). These widely used approaches are powerful tools allowing describing membrane fouling through the estimation of various parameters: resistance due to membrane fouling, reversibility of membrane fouling, main fouling mechanisms, filtration cake thickness and porosity, etc. However, their findings are based on estimation models themselves based on macroscopic scale parameters (flux and pressure) and can be far from the microscopic reality occurring around the membrane surface [1].

In view of the foregoing, advanced techniques allowing fouling characterization directly on the membrane surface have been gaining more and more interest these past years, as they can provide precise information about fouling composition, concentration and location on the membrane. The major techniques used for membrane surface characterization have been reviewed by Johnson et al. [2]. It includes spectroscopic techniques such as ATR-FTIR, Raman and XPS spectroscopy, mainly used to investigate the chemical nature of foulant compounds, their location and even their concentration on the membrane surface [3–5]. Imaging techniques (AFM, SEM, TEM, etc.) are also of great interest for membrane fouling characterization as they can bring information about fouling layer thickness and distribution [1]. The study of the modification of the membrane wetting properties (contact angle) and electrokinetic behavior (electrophoresis, streaming and sedimentation potential measurements) induced by the presence of foulant materials on its surface bring useful information as well [2].

However, most of these techniques mainly focus on the membrane surface characterization. Few studies deal with the characterization of internal fouling, even though this latter is often irreversible and causes severe loss of performances and cleaning overcost. Yeo et al. [6] managed to monitor

external and internal organic fouling deposition on and in a hollow fiber membrane using phase-contact XMI, while 3D optical coherence tomography was successfully used by Trinh et al. [7] to characterize external and internal fouling during microfiltration of oil-in-water emulsions. Similarly, electrochemical impedance spectroscopy has been recently used to identify the main fouling mechanism (external fouling layer or irreversible internal fouling) [8]. Apart from these anecdotal applications, there still is a lack of analytical strategies for internal fouling investigation. Considering the well-known impact of fouling on the membrane charge, the investigation of surface and porous structures zeta potentials may bring useful information for external and internal fouling characterization.

Determining the zeta potential of a membrane provides insight into its surface electrical properties in a given physicochemical environment. It is therefore of great interest when investigating problems of practical relevance such as membrane fouling [9, 10] or ageing [11, 12].

The zeta potential of membranes can be inferred from electrokinetic techniques such as streaming potential and streaming current. From the experimental point of view, the easiest way to perform the electrokinetic characterization of porous membranes is to implement through-pore streaming potential measurements (also known as transversal mode) [13–15]. However, the multilayer structure of commercial membranes used in pressure-driven processes (micro-,ultra- and nano-filtration as well as reverse osmosis) makes the determination of the skin layer properties quite tricky [16–18]. In order to overcome the difficulty inherent in the analysis of through-pore measurements, an alternative measuring method, known as tangential mode and based on the application of the pressure gradient along the membrane skin layer (and not through the membrane thickness) has been proposed and has become the most widely used technique in membrane science [19–22].

When considering tangential electrokinetic measurements, it has been argued that streaming current should be preferred over streaming potential since this latter is likely to be impacted by the extra contribution of the underlying support layer(s) to the overall electrical conductance [23, 24]. Tangential streaming current has been shown to be a reliable technique to highlight the presence of thin coating layers onto the surface of some commercial nanofiltration and reverse osmosis membranes [25]. However, complications have been pointed out when tangential streaming current measurement is applied to porous materials like micro- and ultra-filtration membranes due to the occurrence of a non-negligible streaming current through the membrane porosity[26–28]. This

parasitic contribution to the experimental signal, hereinafter referred as electrokinetic leakage, can be taken into account by applying a protocol consisting in a series of measurements performed by changing the distance between the two membranes samples required for tangential measurements [26–28]. Such a procedure has been successfully applied by Szymczyk *et al.* (2013) to give evidence for the presence of 4-benzyltriphenylphosphonium groups within pores of an ultrafiltration membrane after its functionalization [28].

In this work, we show for the first time that the electrokinetic leakage phenomenon can be used to gain insight into membrane fouling. Notably, we show that electrokinetic leakage can be used as a probe to highlight the occurrence of internal fouling within the porous structure of micro- and ultra-filtration membranes. The methodology followed in this work also enables distinction between fouling onto the membrane surface and within the membrane pores.

2 Theoretical background

Tangential streaming current measurement consists in applying a pressure gradient along a channel formed by two identical membrane samples facing each other and immersed in an electrolyte solution. While the pressure gradient is applied along the membrane skin layers, the solution is forced to move tangentially to the charged surfaces, pulling the excess of mobile ions within the electrical double layers towards the low-pressure side. It results in an electrical current, known as the streaming current (I_s), flowing between the membrane surfaces.

The standard theory implicitly assumes that the channel through which tangential streaming current is measured has impermeable walls. If this condition is fulfilled and the distance between the surfaces of the two membrane samples (h_{ch}) is much larger than the Debye length of the measuring solution, the zeta potential (ζ) can be inferred from the streaming current by means of the well-known Smoluchowski equation:

$$I_s = -\frac{W h_{ch} \varepsilon_0 \varepsilon_r \Delta P}{\eta L} \zeta \qquad (1)$$

where W and L are the channel width and length, respectively, ε_0 the vacuum permittivity (8.854x10^{-12} F m^{-1}), ε_r and η the dielectric constant and the dynamic viscosity of the electrolyte solution, respectively, and ΔP is the pressure difference applied between the channel ends.

Although Eq. (1) is reliable for dense materials, it may break down when applied to ion-permeable materials such as micro- and ultra-filtration membranes, especially if the electrokinetic cell has been designed in such a way that it leaves the membrane support layer(s) exposed to the hydrodynamic flow during streaming current measurements [26, 28]. The reason is that a non-negligible streaming current is likely to flow through the membrane porous structure, which is filled with the measuring solution. This additional streaming current that we shall refer to as "electrokinetic leakage" is not accounted for in Eq. (1), which implicitly assumes that the experimental streaming current only flows along the membrane surfaces. For a given membrane, the occurrence of electrokinetic leakage can be easily confirmed or invalidated by measuring the streaming current for (at least) two different values of h_{ch}. Indeed, in the case of electrokinetic leakage, the (apparent) zeta potential that would be obtained by means of Eq. (1) would become dependent upon the distance between the membrane samples.

Eq. (2) has been proposed by Yaroshchuk and Luxbacher [26] to account for the contribution of electrokinetic leakage (see schematic description given in Fig. 1):

$$I_s^{tot} = I_s^{ch} + 2I_s^{pore} = -\left(\frac{Wh_{ch}\varepsilon_0\varepsilon_r\Delta P}{\eta L}\zeta_{surf} + \frac{2Wh_{mb}^{eff}\varepsilon_0\varepsilon_r\Delta P}{\eta L}\zeta_{pore}\right) \qquad (2)$$

Where I_s^{tot}, I_s^{ch} and I_s^{pore} are the total streaming current (i.e. the current measured experimentally), the streaming current flowing through the channel (i.e. between the membrane surfaces) and the electrokinetic leakage occurring within a single membrane, respectively, ζ_{surf} and ζ_{pore} are the zeta potentials of the membrane surface and inside the membrane porous body, respectively, and h_{mb}^{eff} the effective height where the electrokinetic leakage takes place in a single membrane (it includes the membrane thickness, porosity and tortuosity).

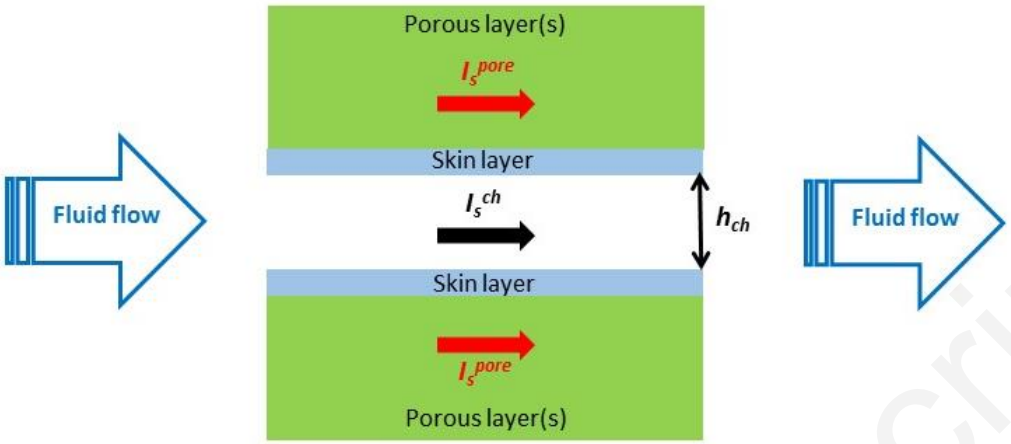

154

155 **Figure 1: Schematic representation of the streaming current distribution when tangential**
156 **electrokinetic measurements are carried out with porous membranes. The streaming current does not**
157 **flow only between the membrane surfaces but also through the membranes porous body. The**
158 **experimental streaming current is then equal to $I_s^{ch} + 2I_s^{pore}$.**

159

160 It is worth mentioning that, unlike Eqs. (1) and (2), the softwares associated with the current
161 commercial electrokinetic analyzers use an arbitrary convention stating that the measured streaming
162 current and the zeta potential(s) are of the same sign. This convention will be used in the rest of this
163 manuscript.

164 According to Eq. (2), the correct value of the zeta potential of the membrane surface can be
165 determined by carrying out a series of streaming current measurements with various channel heights
166 (h_{ch}). Indeed, ζ_{surf} can be obtained from the slope of I_s^{tot} vs. h_{ch} while the total electrokinetic leakage
167 ($2I_s^{pore}$) is given by the y-intercept (the streaming current that would be measured if the two
168 membrane surfaces were brought into contact, i.e. h_{ch} = 0). Eq. (2) also shows that the zeta potential
169 inside the membrane porosity can be determined from the electrokinetic leakage provided if h_{mb}^{eff} is
170 known, which can be achieved by means of additional electric conductance measurements for various
171 h_{ch}. Indeed, considering the system described in Fig. 1 the following expression for the cell
172 conductance (G_{cell}) can be derived [26,28]:

$$G_{cell} = \frac{W}{L}\left(h_{ch}\lambda_0 + 2h_{mb}^{eff}\lambda_{mb}\right) \quad (3)$$

Where λ_0 and λ_{mb} are the electric conductivities of the measuring solution in the channel between the membrane surfaces and inside the membrane pores, respectively.

3 Materials and methods

3.1 Membranes

Two commercial flat-sheet membranes were used in this work: a microfiltration (MF) polyethersulfone (PES) membrane with an average pore diameter of 0.1 µm (Koch, USA) and an ultrafiltration (UF) polyacrylonitrile (PAN) membrane with a molecular weight cut-off (MWCO) of 500kDa (Orelis, France). The following protocol was followed to remove membrane preservatives prior use: sonication first in a 50 v/v % water-ethanol mixture for 10 min followed by sonication in deionized water (DI) water for 10 min (this last step was repeated twice).

3.2 Membrane fouling

3.2.1 Lab-scale fouling experiments

"Upside down" fouling experiments were performed in order to provide the proof of concept of the methodology we propose in this work, which is based on the variation of the electrokinetic leakage occurring in the porous structures of membranes as a result of internal fouling. The protocol is schematically described in Fig. 2. The membrane coupons were fixed at the bottom of a plastic box using adhesive tape, the membrane skin layer facing the bottom of the box (steps 1 and 2 in Fig. 2). Then, commercial sunflower oil was poured onto the surface of the membrane support and homogeneously spread with a paintbrush. Oil was then let diffuse through the membrane (from the support towards the skin layer) for 4 hours at room temperature (step 3). The remaining oil on the support surface was wiped with a tissue paper prior to membrane characterization.

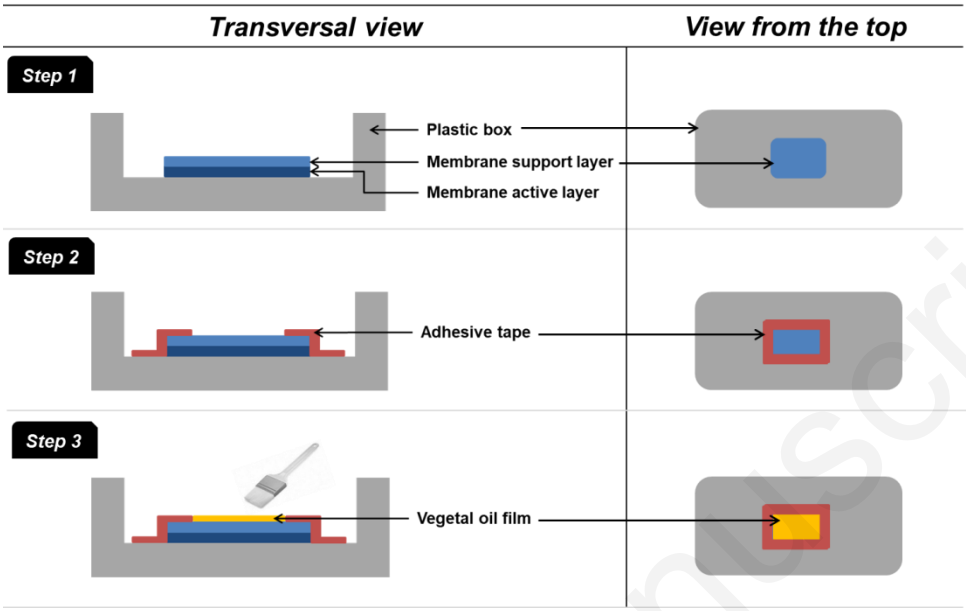

Figure 2: Experimental protocol for upside down fouling of membrane samples by vegetable oil.

3.2.2 Pilot-scale fouling experiments

Pilot-scale fouling experiments were performed using a cross-flow filtration module (Rayflow X100, Orelis-Novasep, France) with a filtration area close to 130 cm^2. The feed cross-flow circulation was ensured by a peristaltic pump (ref 520S IP31, Watson-Marlow, USA), the cross-flow velocity being around 0.4 $m.s^{-1}$. Permeation through the membrane was ensured by applying a constant transmembrane pressure difference (TMP) adjusted with a back-pressure valve. Two pressure sensors placed at the module inlet and outlet on the retentate side allowed TMP monitoring and adjustment [29]. Before measurements, the membranes were first cleaned by successive filtrations of alkali solutions according to the following order: mixture of 0.1 $g.L^{-1}$ NaOH and 0.02 $g.L^{-1}$ NaClO solution at 30°C (pH ~ 10-11), followed by 2 $g.L^{-1}$ commercial Ultrasil 110 solution (Ecolab, France) at 45°C. Between each cleaning step, membranes were carefully rinsed in order to remove the remaining chemicals. To this end, successive filtrations of DI water (30°C) without permeate and retentate recirculation and under constant pressure of 0.2 bar were performed until the permeate reached the pH of DI water. At the end of the cleaning step, membranes were compacted by DI water

filtration at constant TMP (2 bar) and constant temperature (30±1°C) until a steady state water flux was reached (± 5%). The evolution of the permeate flux during the filtration process was measured by collecting the permeate in a beaker placed on an electronic scale (model XL1200C, Precisa, Switzerland).

After membrane compaction, DI water filtration pressure-stepping experiments (5 pressure steps from 0.2 to 1.0 bar) were carried out in order to determine the 30°C water permeability of each coupon.

Fouling experiments were further conducted using a 2% oil-in-water emulsion as the foulant feed (~ 2 liters). It was used by some of us in a previous study as a model system representative of the supernatant of a concentrated pretreated culture of *Parachlorella kessleri* microalgae, after bead milling and separation of the cell fragments by centrifugation [29,30]. The aqueous phase had a pH of 7.4 and a conductivity of 790 µS cm^{-1} and the lipid phase consisted in a mixture of vegetable oils containing 70 wt% of neutral lipids and 30 wt% of polar lipids [29]. Fouling experiments were carried out at two TMP (0.2 and 1.0 bar) so as to get different levels of fouling. Experiments were stopped when a volume reduction ratio of 2 was achieved and the membranes were further rinsed by two successive DI water filtrations under a TMP of 0.2 bar for 15 minutes in order to remove the reversible part of fouling.

3.3 Membrane characterization: Tangential streaming current

Electrokinetic measurements were performed with a Surpass electrokinetic analyzer (Anton Paar GmbH) equipped with an adjustable-gap cell requiring two membrane samples (each one 2 x 1 cm) [28]. For all experiments, the membranes were positioned in the adjustable-gap cell with their skin layers facing each other (as shown schematically in Fig. 1). Experiments were performed at T=22±2 °C with 500 mL of a 0.001 M KCl solution, the pH of which was adjusted in the range 4.50 – 5.00 with a 0.05 M HCl solution and kept constant within ± 0.05 throughout the course of the experiment. Prior to measurements, the solution was circulated through the channel for *ca.* 2 h to allow the sample equilibration. After equilibration, the streaming current was measured and recorded for increasing pressure differences (ΔP) up to 300 mbar. Measurements were repeated by progressively decreasing

the distance between the membrane samples (h_{ch}) from ~100 µm to ~40 µm by means of the micrometric screws of the adjustable-gap cell.

For some experiments, the electrical conductance of the adjustable-gap cell was also measured (for various values of h_{ch}) in order to evaluate the effective height where the electrokinetic leakage takes place in the membrane (h_{mb}^{eff}). For these additional measurements, a more concentrated KCl solution (0.1 M) was used in order to minimize the impact of the electrical double layers on the electrical conductivity inside the membrane pores [28].

4 Results

4.1 Proof of concept

In a preliminary work, the UF PAN membrane was first fouled according to the "upside down" fouling protocol described in section 3.2.1 and schematically shown in Fig. 2. Next, two membrane samples were positioned in the adjustable-gap cell of the electrokinetic analyzer with their skin layers facing each other (as shown schematically in Fig. 1). For all experiments, a linear variation was observed between the applied pressure and the resulting streaming current, making it possible to unambiguously define the streaming current coefficient as the slope of the I_s^{tot} vs ΔP plots. Fig. 3 shows the variation of the streaming current coefficient as function of the distance between the membrane samples in the adjustable-gap cell (h_{ch}). As expected from Eq. (2), a linear variation was observed for both new and fouled membrane samples.

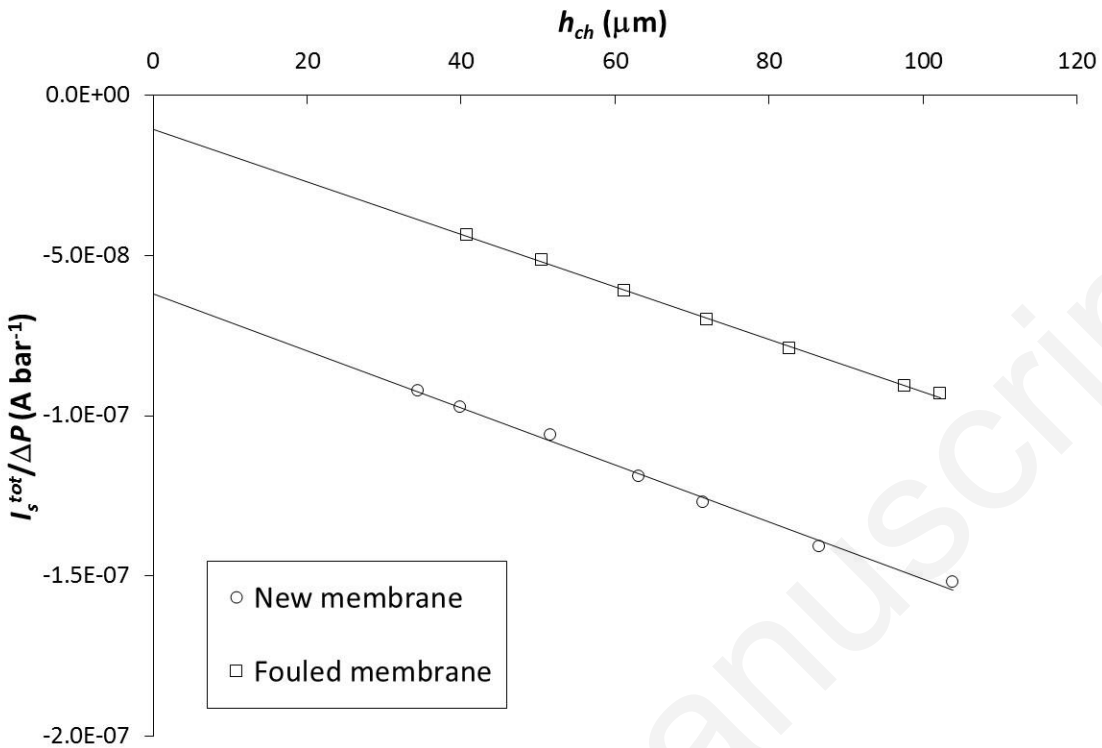

Figure 3: Streaming current coefficient of the pristine and fouled PAN membranes as function of the distance between the samples; measuring solution: 0.001 M KCl solution at pH 4.50 ±0.05.

Extrapolating the streaming current coefficient of the pristine membrane down to h_{ch} = 0 (i.e. membrane surfaces in contact with no longer a channel in between) gives evidence of the electrokinetic leakage phenomenon since the y-intercept differs from zero, as shown by Eq. (2). It was found to be -6.2x10^{-8} A.bar^{-1}, which represents 40% of the experimental signal ($I_s^{tot}/\Delta P$) measured by setting the distance between the samples at 100 μm and up to 65% of the experimental signal if h_{ch} is set at 40 μm. In the Supplementary Information of this manuscript, the reader can find additional measurements obtained with a track-etched membrane (Fig. S1). As expected, no electrokinetic leakage occurred since track-etched membranes have non-interconnected pores, thus preventing any tangential flow through the porous structure.

Interestingly, an almost six-fold decrease in the magnitude of the electrokinetic leakage was obtained after letting the support layer of the PAN membrane in contact with sunflower oil for four hours as described in section 3.2.1. These results can be explained as follows. With the pristine membranes,

the electrokinetic leakage phenomenon can take place because the membrane pores are filled with the electrolyte solution required for electrokinetic measurements, which creates ion-conductive pathways through which a part of the streaming current, $2I_s^{pore}$ in Eq. (2), can flow (see Fig. 4a); the magnitude of the electrokinetic leakage would increase with the membrane thickness, porosity, hydrophilicity and pore surface charge. Because of the hydrophobic character of oil, these conductive pathways are progressively clogged as oil penetrates into the membrane pores (Fig. 4b), which results in a weaker electrokinetic leakage as reported in Fig. 3.

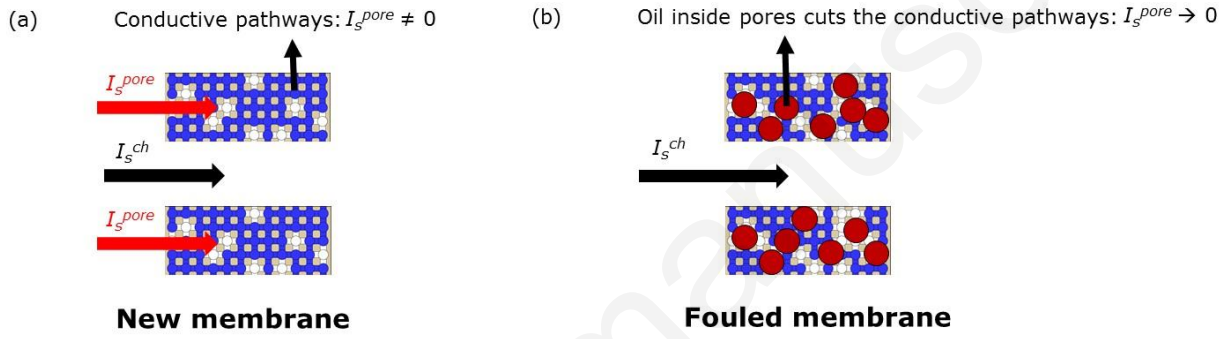

Figure 4: Schematic representation of (a) open conductive pathways allowing electrokinetic leakage through the membrane porosity and (b) clogged conductive pathways leading to electrokinetic leakage disappearance.

It is worth noting in Fig. 3 that the same slope was obtained in the electrokinetic response of both PAN membrane coupons. According to Eq. (2), this results means that the zeta potential of the skin layer surface (ζ_{surf}) was not impacted after membrane fouling. Otherwise stated, it means that oil entered the membrane pores from the support layer side but did not cross the membrane skin layer.

These results show that the proposed methodology makes it possible to separate the contribution of surface and internal fouling.

As stated in section 2, the effective height where the electrokinetic leakage takes place in a single membrane (h_{mb}^{eff}) can be estimated by means of additional electric conductance measurements. Fig. 5 shows the variation of the cell conductance (G_{cell}) as function of h_{ch}. As predicted by Eq. (3), a linear variation of G_{cell} with h_{ch} was obtained for both new and fouled PAN membranes. A concentrated

299 solution (0.1 M KCl) was used to minimize the impact of the electrical double layers on the electrical
300 conductivity inside the membrane pores and to reasonably assume $\lambda_{mb} \approx \lambda_0$[28]. The h_{mb}^{eff} values for
301 both membranes were inferred from the y-intercept according to Eq. (3). For the pristine membrane,
302 h_{mb}^{eff} was found to be about 40 μm while it fell down to 2 μm for the fouled membrane, thus confirming
303 that the presence of oil inside the membrane pores cut the conduction pathways responsible for the
304 electrokinetic leakage phenomenon.

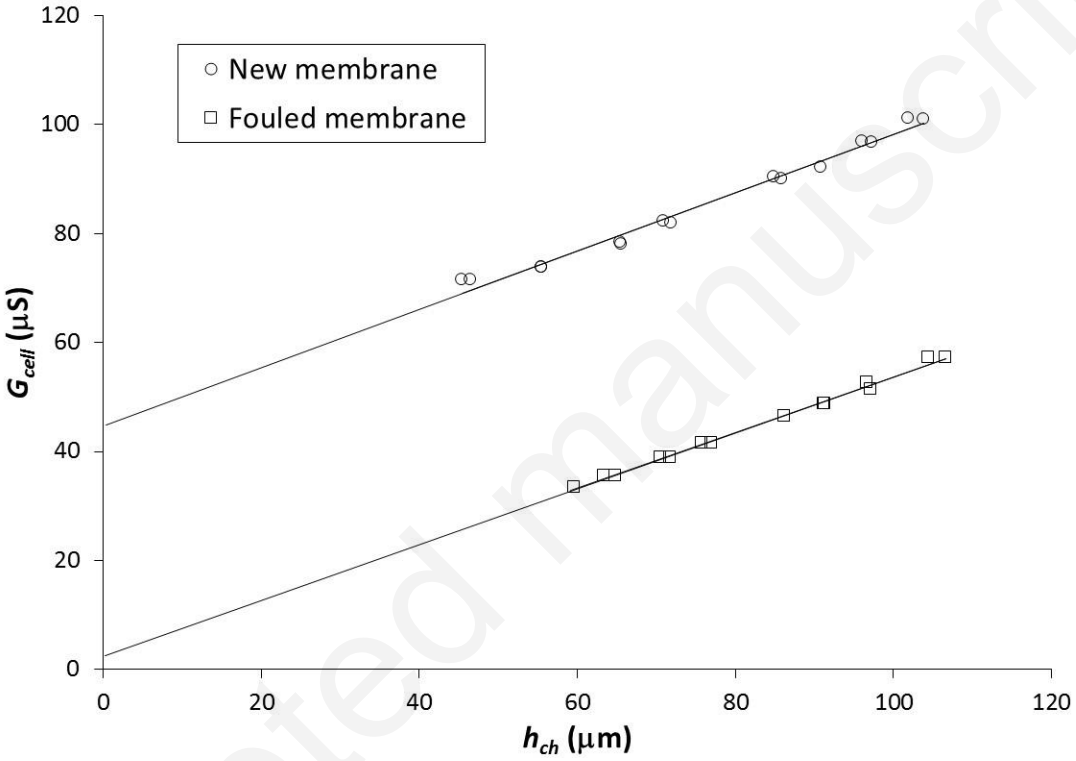

305

306 **Figure 5: Cell conductance measured with the PAN membranes as a function of the distance between**
307 **the samples; measuring solution: 0.1 M KCl solution at pH 4.50 ±0.05.**

308

309 ## 4.2 Application to oil-in-water emulsion filtration

310 Pilot-scale filtration experiments were then conducted on the 2% oil-in-water emulsion using MF PES
311 and UF PAN membranes. Fig. 6 shows the variation of the streaming current coefficient of the MF PES
312 membrane as function of the distance between the membrane samples in the adjustable-gap cell (h_{ch}).

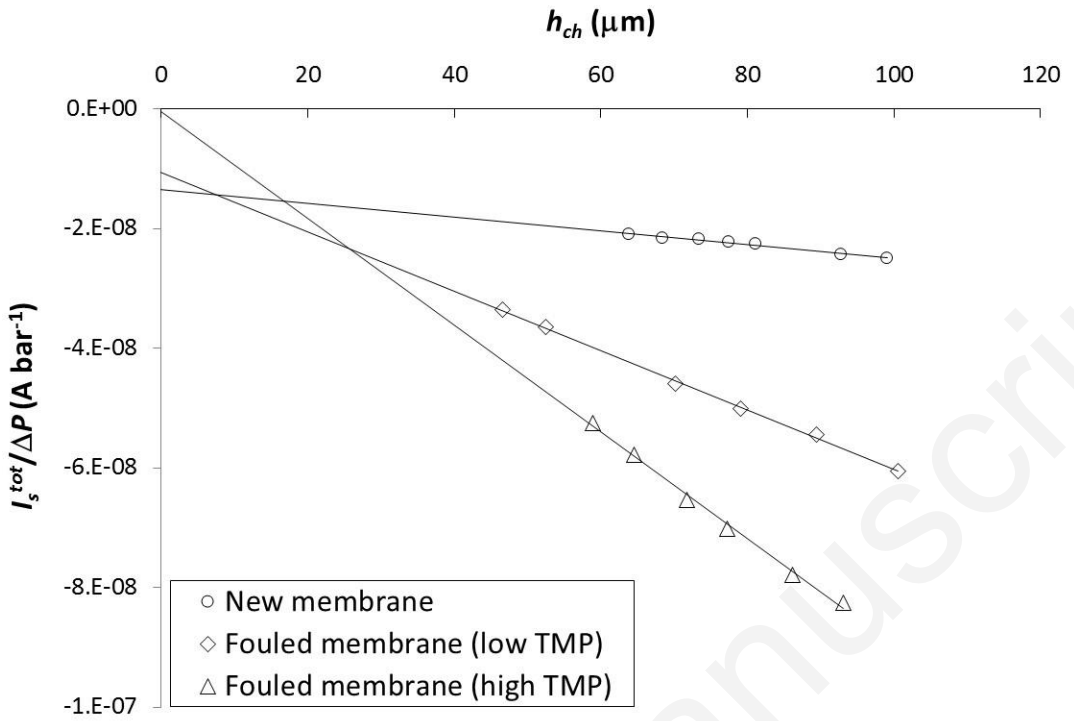

313

314 **Figure 6: Streaming current coefficient of the pristine and fouled PES membranes as function of the**
315 **distance between the samples; measuring solution: 0.001 M KCl solution at pH 5.00 ±0.05.**

316

317 Different electrokinetic responses were obtained for the pristine membrane and the membranes
318 fouled by filtering the 2% oil-in-water emulsion described in section 3.2.2.

319 The slope of the electrokinetic response was found to increase with fouling, being even steeper after
320 filtration at high TMP (1 bar). Since the slope of the $I_s{}^{tot}/\Delta P$ vs h_{ch} plot is proportional to ζ_{surf} (see Eq.
321 (2)), it means that (i) the zeta potential of the foulant was higher than that of the bare membrane
322 surface and (ii) the coverage of the PES membrane surface by the oil droplets (surface fouling)
323 increased by applying a higher TMP. The values of ζ_{surf} can be straightforwardly deduced from Eq.
324 (2) and are collected in Table 1.

325 A slight decrease in the electrokinetic leakage is observed after filtration of the emulsion at low TMP
326 (0.2 bar). On the other hand, the electrokinetic leakage almost vanished after filtration at 1 bar (it was
327 divided by a factor of 34 compared with the pristine membrane). These results indicate that a higher

TMP favored the penetration of the oil droplets into the porous structure of the 0.1 μm PES membrane.

Table 1: Surface zeta potentials(ζ_{surf}) of the various membranes inferred from Eq. (2).

Membrane	Membrane surface zeta potential (mV)		
	New	*Fouled (low TMP)*	*Fouled (high TMP)*
PES 0.1 μm	-2.9 ± 0.9	-13.0 ± 0.6	-23.1 ± 1.4
PAN 500 kDa	-35.1 ± 1.0	-26.1 ± 2.9	-26.8 ± 2.3

It can be noted that the standard Smoluchowski equation (Eq. (1)) could be used with confidence to compute the surface zeta potential of the PES membrane fouled at high TMP since the electrokinetic leakage phenomenon was suppressed under these operating conditions: the surface zeta potential determined from Eq. (1) with h_{ch} = 100 μm and from Eq. (2) are -23.2 mV and -23.1 mV, respectively. However it would overestimate the surface zeta potential of the new PES membrane and the membrane fouled at low TMP by 117 % and 21 %, respectively (still considering data for h_{ch} = 100 μm in Eq. (1)).

A different behavior was observed with the 500 kDa UF PAN membrane. Indeed, as shown in Fig. 7, the impact of the TMP on both the external and internal fouling was marginal since the electrokinetic response (slope and y-intercept) of membranes fouled at low and high TMP were found to be very close.

The surface of the PAN membrane was found to be more negatively charged than the PES membrane (see Table 1). The slope of the electrokinetic reponse (and thus the surface zeta potential) was found to slighty decrease after fouling, unlike what was observed with the PES membrane for which a strong increase was reported (Fig. 6). It means that the foulant species from the emulsion were less negatively charged than the pristine PAN membrane. The surface zeta potentials of both the new and fouled PAN membranes are given in Table 1.

The PAN membrane appeared to be less prone to internal fouling by the oil-in-water emulsion than the PES membrane since the electrokinetic leakage occurring in the PAN and PES membranes decreased by a factor of 1.7 and 34, respectively, after fouling at high TMP. It results from to the more open porous structure of the MF PES membrane compared with the UF PAN membrane along with the more hydrophobic character of PES [10, 11] favoring interactions with the oil droplets.

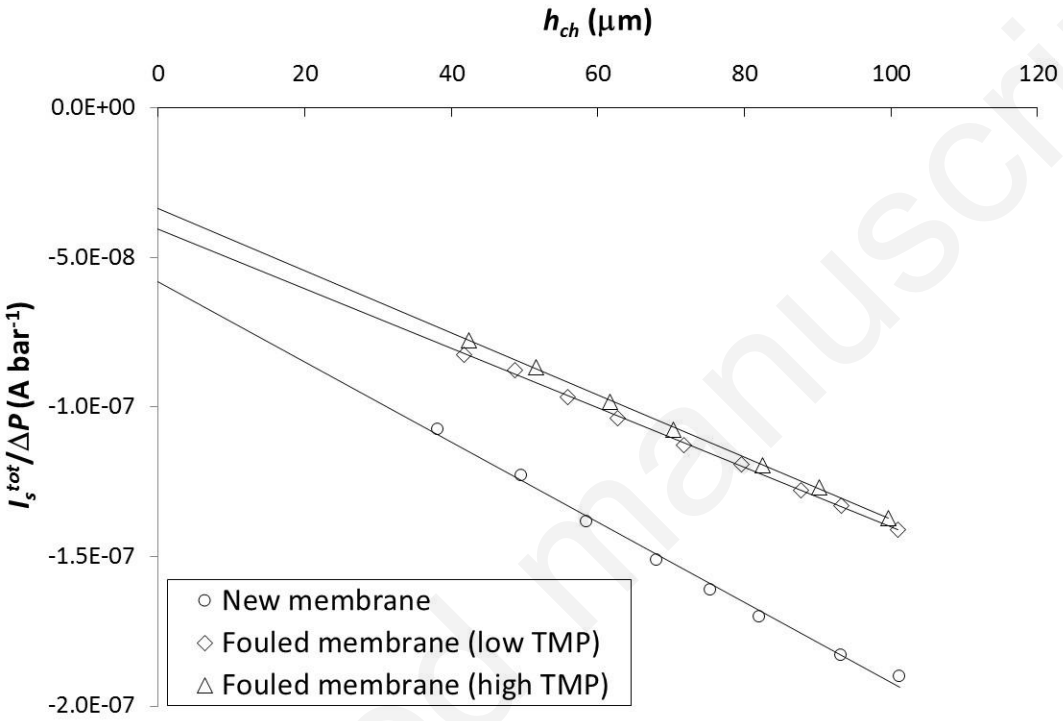

Figure 7: Streaming current coefficient of the pristine and fouled PAN membranes as function of the distance between the samples; measuring solution: 0.001 M KCl solution at pH 5.00 ±0.05.

Interestingly, ζ_{surf} for the fouled PAN membranes and the PES membrane fouled at high TMP were found to be very close: -26.1, -26.8 and -23.1 mV for the PAN membrane fouled at low TMP, the PAN membrane fouled at high TMP and the PES membrane fouled at high TMP, respectively. Since the bare PAN and PES membranes had substantially different ζ_{surf} (-35.1 and -2.9 mV, respectively), this finding suggests that (i) the surface of both membranes was fully covered by foulant species from the emulsion and (ii) these foulant species develop an electrokinetic charge density in the

364 physicochemical environment considered in this study (0.001 M KCl at pH 5), which is characterized
365 by a zeta potential in the range from ~ -20 mV to ~ -30 mV.

366 Additional electrophoretic light scattering measurements were performed with the emulsion diluted
367 1000 times in a 0.001 M KCl solution at pH 5. The zeta potential of the emulsion droplets was found
368 to be -25.7 ± 1.1 mV, which confirms that the PES membrane surface was fully covered after filtration
369 at high TMP while that of the PAN membrane was covered even at low TMP.

370

371 5 Conclusion

372 The electrokinetic leakage, which is the part of the streaming current that flows through the porosity
373 of a membrane when tangential electrokinetic measurements are carried out, is a parasitic
374 phenomenon that makes more tedious the accurate determination of the surface zeta potential.
375 Nonetheless, since this parasitic contribution is sensitive to local changes inside the membrane
376 porosity it is likely to provide useful information when investigating problems of practical relevance.
377 In this study, we showed for the first time that electrokinetic leakage can serve as a probe for
378 detecting internal fouling in MF and UF membranes, taking lipidic fouling as example. Notably, it was
379 used to highlight the substantial impact of the TMP on the internal fouling of a MF PES membrane
380 caused by filtration of an oil-in-water emulsion. On the other hand, almost no impact of the TMP was
381 noticed in the case of a UF PAN membrane with narrower pores. Moreover, the experimental protocol
382 implemented here to quantify the electrokinetic leakage phenomenon allowed to distinguish between
383 the contribution of internal fouling and that of external (surface) fouling.

384 This paper offers new prospects for tangential electrokinetic measurements by providing an
385 innovative methodology for the characterization of internal fouling. These findings could find useful
386 application in MF and UF processes for which internal fouling is often responsible of severe
387 productivity decrease and laborious cleaning procedures. Moreover, in view of the vast volumes of
388 oily wastewater produced in various industrial fields (microalgae, food and beverages, oil and gas,
389 metal processing, etc.), the characterization of membrane fouling during oil-in-water emulsions
390 treatment is a key challenge for the development of cost-effective and eco-friendly processing
391 involving membranes filtration.

Interestingly, the methodology proposed in this work is not restricted to membrane fouling studies and it could be applied straightforwardly to other topics of membrane science including membrane functionalization and membrane degradation (physical or chemical ageing). A limitation of this method is that it requires varying the spacing between the membranes, which makes it difficult to apply it on-line with existing membrane modules.

6 Acknowledgements

Cédric Brossard (Malvern Panalytical) is gratefully acknowledged for electrophoretic light scattering measurements. This work was supported by GIS Europôle Mer, France (Sciences et Ingénieries Marines, 2016-2017), Université de Bretagne Loire, ADEME and the Challenge Food For Tomorrow/Cap Aliment, Pays de la Loire, France.

7 Bibliography

[1] G. Rudolph, T. Virtanen, M. Ferrando, C. Güell, F. Lipnizki, M. Kallioinen, A review of in situ real-time monitoring techniques for membrane fouling in the biotechnology, biorefinery and food sectors, J. Membr. Sci. 588 (2019) 117221. doi:10.1016/j.memsci.2019.117221.

[2] D.J. Johnson, D.L. Oatley-Radcliffe, N. Hilal, State of the art review on membrane surface characterisation: Visualisation, verification and quantification of membrane properties, Rev. Res. Dev. Desalination. 434 (2018) 12–36. doi:10.1016/j.desal.2017.03.023.

[3] D. Delaunay, M. Rabiller-Baudry, J.M. Gozálvez-Zafrilla, B. Balannec, M. Frappart, L. Paugam, Mapping of protein fouling by FTIR-ATR as experimental tool to study membrane fouling and fluid velocity profile in various geometries and validation by CFD simulation, Euromembrane 2006. 47 (2008) 1106–1117. doi:10.1016/j.cep.2007.12.008.

[4] M. Rabiller-Baudry, L. Bégoin, D. Delaunay, L. Paugam, B. Chaufer, A dual approach of membrane cleaning based on physico-chemistry and hydrodynamics: Application to PES membrane of dairy industry, 10th Fr. Congr. Chem. Eng. 47 (2008) 267–275. doi:10.1016/j.cep.2007.01.026.

[5] M.J. Luján-Facundo, J.A. Mendoza-Roca, B. Cuartas-Uribe, S. Álvarez-Blanco, Evaluation of cleaning efficiency of ultrafiltration membranes fouled by BSA using FTIR–ATR as a tool, J. Food Eng. 163 (2015) 1–8. doi:10.1016/j.jfoodeng.2015.04.015.

[6] A. Yeo, P. Yang, A.G. Fane, T. White, H.O. Moser, Non-invasive observation of external and internal deposition during membrane filtration by X-ray microimaging (XMI), J. Membr. Sci. 250 (2005) 189–193. doi:10.1016/j.memsci.2004.10.035.

[7] T.A. Trinh, W. Li, Q. Han, X. Liu, A.G. Fane, J.W. Chew, Analyzing external and internal membrane fouling by oil emulsions via 3D optical coherence tomography, J. Membr. Sci. 548 (2018) 632–640. doi:10.1016/j.memsci.2017.10.043.

[8] M.C. Martí-Calatayud, S. Schneider, M. Wessling, On the rejection and reversibility of fouling in ultrafiltration as assessed by hydraulic impedance spectroscopy, J. Membr. Sci. 564 (2018) 532–542. doi:10.1016/j.memsci.2018.07.021.

[9] J. Benavente, G. Jonsson, Effect of adsorbed protein on the hydraulic permeability, membrane and streaming potential values measured across a microporous membrane, Colloids Surf. Physicochem. Eng. Asp. 138 (1998) 255–264. doi:10.1016/S0927-7757(97)00119-2.

[10] L. Marbelia, M. Mulier, D. Vandamme, K. Muylaert, A. Szymczyk, I.F.J. Vankelecom, Polyacrylonitrile membranes for microalgae filtration: Influence of porosity, surface charge and microalgae species on membrane fouling, Algal Res. 19 (2016) 128–137. doi:10.1016/j.algal.2016.08.004.

[11] Y. Hanafi, A. Szymczyk, M. Rabiller-Baudry, K. Baddari, Degradation of Poly(Ether Sulfone)/Polyvinylpyrrolidone Membranes by Sodium Hypochlorite: Insight from Advanced Electrokinetic Characterizations, Environ. Sci. Technol. 48 (2014) 13419–13426. doi:10.1021/es5027882.

[12] Y. Hanafi, P. Loulergue, S. Ababou-Girard, C. Meriadec, M. Rabiller-Baudry, K. Baddari, A. Szymczyk, Electrokinetic analysis of PES/PVP membranes aged by sodium hypochlorite solutions at different pH, J. Membr. Sci. 501 (2016) 24–32. doi:10.1016/j.memsci.2015.11.041.

[13] M. Nyström, A. Pihlajamäki, N. Ehsani, Characterization of ultrafiltration membranes by simultaneous streaming potential and flux measurements, J. Membr. Sci. 87 (1994) 245–256. doi:10.1016/0376-7388(94)87031-4.

[14] I.H. Huisman, P. Prádanos, A. Hernández, Electrokinetic characterisation of ultrafiltration membranes by streaming potential, electroviscous effect, and salt retention, J. Membr. Sci. 178 (2000) 55–64. doi:10.1016/S0376-7388(00)00479-8.

[15] M. Sbaï, P. Fievet, A. Szymczyk, B. Aoubiza, A. Vidonne, A. Foissy, Streaming potential, electroviscous effect, pore conductivity and membrane potential for the determination of the surface potential of a ceramic ultrafiltration membrane, J. Membr. Sci. 215 (2003) 1–9. doi:10.1016/S0376-7388(02)00553-7.

[16] A. Szymczyk, C. Labbez, P. Fievet, B. Aoubiza, C. Simon, Streaming potential through multilayer membranes, AIChE J. 47 (2001) 2349–2358. doi:10.1002/aic.690471019.

[17] A.E. Yaroshchuk, Y.P. Boiko, A.L. Makovetskiy, Filtration Potential across Membranes Containing Selective Layers, Langmuir. 18 (2002) 5154–5162. doi:10.1021/la025503s.

[18] P. Fievet, M. Sbaï, A. Szymczyk, Analysis of the pressure-induced potential arising across selective multilayer membranes, J. Membr. Sci. 264 (2005) 1–12. doi:10.1016/j.memsci.2005.04.011.

[19] D. Möckel, E. Staude, M. Dal-Cin, K. Darcovich, M. Guiver, Tangential flow streaming potential measurements: Hydrodynamic cell characterization and zeta potentials of carboxylated polysulfone membranes, J. Membr. Sci. 145 (1998) 211–222. doi:10.1016/S0376-7388(98)00077-5.

[20] P. Fievet, M. Sbaï, A. Szymczyk, C. Magnenet, C. Labbez, A. Vidonne, A New Tangential Streaming Potential Setup for the Electrokinetic Characterization of Tubular Membranes, Sep. Sci. Technol. 39 (2004) 2931–2949. doi:10.1081/SS-200028652.

[21] V.T. Do, C.Y. Tang, M. Reinhard, J.O. Leckie, Degradation of Polyamide Nanofiltration and Reverse Osmosis Membranes by Hypochlorite, Environ. Sci. Technol. 46 (2012) 852–859. doi:10.1021/es203090y.

[22] S. Liu, C. Wu, X. Hou, J. She, S. Liu, X. Lu, H. Zhang, S. Gray, Understanding the chlorination mechanism and the chlorine-induced separation performance evolution of polypiperazine-amide nanofiltration membrane, J. Membr. Sci. 573 (2019) 36–45. doi:10.1016/j.memsci.2018.11.071.

[23] A. Yaroshchuk, V. Ribitsch, Role of Channel Wall Conductance in the Determination of ζ-Potential from Electrokinetic Measurements, Langmuir. 18 (2002) 2036–2038. doi:10.1021/la015557m.

[24] P. Fievet, M. Sbaï, A. Szymczyk, A. Vidonne, Determining the ζ-potential of plane membranes from tangential streaming potential measurements: effect of the membrane body conductance, J. Membr. Sci. 226 (2003) 227–236. doi:10.1016/j.memsci.2003.09.007.

[25] E. Idil Mouhoumed, A. Szymczyk, A. Schäfer, L. Paugam, Y.H. La, Physico-chemical characterization of polyamide NF/RO membranes: Insight from streaming current measurements, J. Membr. Sci. 461 (2014) 130–138. doi:10.1016/j.memsci.2014.03.025.

[26] A. Yaroshchuk, T. Luxbacher, Interpretation of Electrokinetic Measurements with Porous Films: Role of Electric Conductance and Streaming Current within Porous Structure, Langmuir. 26 (2010) 10882–10889. doi:10.1021/la100777z.

[27] S. Déon, P. Fievet, C. Osman Doubad, Tangential streaming potential/current measurements for the characterization of composite membranes, J. Membr. Sci. 423–424 (2012) 413–421. doi:10.1016/j.memsci.2012.08.038.

[28] A. Szymczyk, Y.I. Dirir, M. Picot, I. Nicolas, F. Barrière, Advanced electrokinetic characterization of composite porous membranes, J. Membr. Sci. 429 (2013) 44–51. doi:10.1016/j.memsci.2012.11.076.

[29] L. Villafaña-López, E.C. Rivera, S. Liu, E. Couallier, M. Frappart, Shear-enhanced membrane filtration of model and real microalgae extracts for lipids recovery in biorefinery context, Bioresour. Technol. (2019) 121539. doi:10.1016/j.biortech.2019.121539.

[30] E. Clavijo Rivera, V. Montalescot, M. Viau, D. Drouin, P. Bourseau, M. Frappart, C. Monteux, E. Couallier, Mechanical cell disruption of Parachlorella kessleri microalgae: Impact on lipid fraction composition, Bioresour. Technol. 256 (2018) 77–85. doi:10.1016/j.biortech.2018.01.148.

Supplementary Information

Electrokinetic leakage as a tool to probe internal fouling in MF and UF membranes

C. Rouquié[1,2,3], S. Liu[2,4], M. Rabiller-Baudry[1], A. Riaublanc[3], M. Frappart[2], E. Couallier[2]*, A. Szymczyk[1]*

[1] Univ Rennes, CNRS, ISCR (Institut des Sciences Chimiques de Rennes) – UMR 6226, F-35000 Rennes, France

[2]CNRS, GEPEA, Université de Nantes, 37 Boulevard de l'université, BP 406, 44602Saint-Nazaire cedex, France

[3]INRA, BIA, Rue de la Géraudière, BP 71627, 44 316 Nantes Cedex 3, France

[4]ADEME, 20 avenue du Grésillé, BP90406, 49004 Angers cedex 01, France

*Corresponding authors: anthony.szymczyk@univ-rennes1.fr, estelle.couallier@univ-nantes.fr

Number of pages: 2

Number of Figures: 1

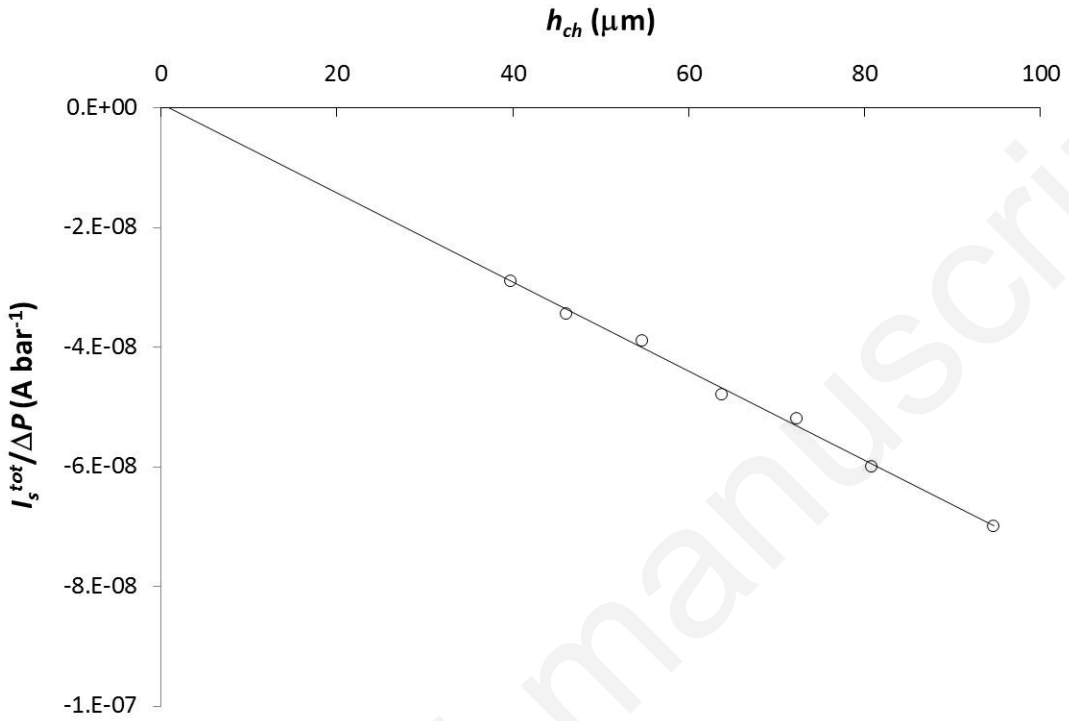

Figure S1: Streaming current coefficient of a track-etched membrane as function of the distance between the samples; measuring solution: 0.001 M KCl solution at pH 5.00 ±0.05.